Hawking radiation for a Proca field in *D* dimensions

Carlos Herdeiro,[*] Marco O. P. Sampaio,[†] and Mengjie Wang[‡]

Departamento de Física da Universidade de Aveiro and I3N Campus de Santiago, 3810-183 Aveiro, Portugal
(Received 4 November 2011; published 4 January 2012)

We study the wave equation of a massive vector boson in the background of a *D*-dimensional Schwarzschild black hole. The mass term introduces a coupling between two physical degrees of freedom of the field, and we solve the resulting system of ordinary differential equations numerically, without decoupling. We show how to define decoupled transmission factors from an **S** matrix and compute them for various modes, masses, and space-time dimensions. The mass term lifts the degeneracy between transverse modes, in *D* = 4, and excites the longitudinal modes, in particular, the *s* wave. Moreover, it increases the contribution of waves with larger ℓ, which can be dominant at intermediate energies. The transmission factors are then used to obtain the Hawking fluxes in this channel. Our results alert for the importance of modeling the longitudinal modes correctly, instead of treating them as decoupled scalars as they are in current black hole event generators; thus, they can be used to improve such generators for phenomenological studies of TeV gravity scenarios.

PACS numbers: 04.50.−h, 04.60.Bc, 04.62.+v, 04.70.Dy

I. INTRODUCTION

Separation of variables and decoupling of degrees of freedom are two key properties in the study of wave equations in gravitational backgrounds. Most remarkably, the gravitational perturbations of the Kerr black hole both separate and decouple, as first exhibited in the celebrated work of Teukolsky [1], which allowed to show linear stability of the Kerr solution. Introducing charge or considering higher dimensions, for instance, seems to spoil such exceptionality; indeed, gravitational perturbations do not seem separable in either the four dimensional Kerr-Newman background [2] or the higher dimensional Myers-Perry background [3].

Failure to achieve separation of variables or to decouple individual degrees of freedom typically leads to the problem of solving sets of coupled ordinary differential equations (ODEs).[1] In the absence of analytic strategies, a full solution of the problem can only be obtained numerically. Surprisingly, numerical solutions for such (common) problems seem to be essentially unexplored, in the context of Hawking radiation, in contrast to the vast literature concerning fully decoupled and separable problems. Perhaps the reason is connected to the problem of quantization, which is usually straightforward when a complete set of decoupled modes is available. We will show, however, that coupled systems (of the type considered herein) may be treated similarly using an **S**-matrix–type formalism which allows decoupling in the asymptotic regions.

In this paper, we shall consider a wave equation, which separates but does not decouple, in the background of a

D-dimensional spherically symmetric Schwarzschild black hole [4]: the massive spin 1, or Proca, field. In contrast, observe that the Maxwell field in the *D* = 4 Schwarzschild background has two physical decoupled polarizations. Introducing the mass term, the spin 1 field gains a longitudinal polarization, and two of the physical degrees of freedom cannot be decoupled. In higher dimensions, the situation is similar, when set in appropriate variables. We shall solve the wave equation for the Proca field in the *D*-dimensional Schwarzschild background numerically to obtain a scattering matrix. This will allow us to define transmission factors as well as the Hawking radiation flux of vector bosons from such black holes.

The technique used herein can, in principle, be applied to other problems of test field wave equations or studies of gravitational perturbations, including the computation of quasinormal modes.[2] Our choice of the Proca field was primarily due to its simplicity, but most importantly for its phenomenological interest to TeV scale gravity scenarios [7–10]. In such scenarios, scattering processes with center of mass energy well above the fundamental Planck scale should be dominated by classical gravitational interactions [11]. Moreover, for sufficiently small impact parameter, black holes should form in particle collisions, as made manifest by numerical evidence [12]. This was predicted by early trapped surface calculations [13] in *D* ≥ 4, which gives bounds on the gravitational radiation emitted; the latter was also estimated through perturbation theory studies of head-on collisions of shock waves in *D* = 4. In *D* > 4, recent results have produced improved semi-analytic estimates within perturbation theory [14]. Other estimates may be obtained from high energy black hole collisions in numerical relativity. The first results for

---

[*]herdeiro@ua.pt
[†]msampaio@ua.pt
[‡]mengjie.wang@ua.pt
[1]Nonseparability leads to partial differential equations but these may be discretized to systems of ODEs.

---

[2]See [5,6] for studies of quasinormal modes where similar coupled systems have been considered.

numerical collisions of higher dimensional black holes have been released in [15–17], based on the frameworks in [18,19]. These black holes would then decay via Hawking radiation [20] and leave observable signatures [21], such as large multiplicity of jets or large transverse momentum, and considerable missing energy due to gravitational wave emission. To better understand and model these scenarios, as well as to improve the phenomenology of black hole event generators such as CHARYBDIS2 [22] and BLACKMAX [23], currently in use at the Large Hadron Collider, it is important to understand the Hawking radiation from higher dimensional black holes. This is especially relevant because the first experimental tests of trans-Planckian gravity scenarios are under way [24–26], and therefore improving their phenomenology is very timely. The computation of Hawking radiation for such models requires solving the wave equation for various fields with different spins, masses, and charges in these black hole backgrounds. In particular, the Proca field in the D-dimensional Schwarzschild background has not been considered up to now.

Our results exhibit distinctive features as we introduce the mass term, such as the lifting of the degeneracy of the two transverse modes in four dimensions, the appearance of longitudinal mode contributions (absent for Maxwell's theory) and, in particular, the s wave. One feature that appears not to have been discussed in the literature is that in four and five space-time dimensions, the transmission factor has a nonvanishing value in the limit of zero spatial momentum. We will also find the expected suppression with M, but perhaps the most relevant feature is to notice the increasing importance of the longitudinal modes and larger ℓ partial waves. Moreover, the precise contribution of the longitudinal modes deviates from simple models that have been used in the aforementioned Monte Carlo event generators to produce phenomenological data, providing our results with phenomenological interest in this context.

This paper is organized as follows. In Sec. II we explain how to decompose the Proca field equation in a generic factorizable background geometry consisting of a warped product of an m-dimensional space with an n-dimensional Einstein space, using the harmonic functions of the Einstein space. In Sec. III we specialize the equations of motion to a D-dimensional Schwarzschild background and present an appropriate set of independent degrees of freedom of the Proca field. We then study the asymptotic and near horizon behavior of the coupled radial equations, which is required to impose the boundary conditions and to define the scattering matrix. In Sec. IV we discuss how the scattering matrix is used to compute the transmission factor and the Hawking spectrum. In Sec. V we discuss the numerical method and results, and we conclude with a discussion in Sec. VI. Some technical relations are left to the Appendix.

II. THE PROCA EQUATIONS IN EINSTEIN SYMMETRIC SPACETIMES

In this section, we present the wave equations for a Proca field which may be complex and charged under a $U(1)$ electromagnetic field. This covers the effective fields describing the Z and W particles in the standard model (SM) of particle physics, the former being a neutral Proca field and the latter being an electromagnetically charged Proca field. In the next section, we will specialize to the neutral case which we want to study in detail. The Lagrangian is

$$\mathcal{L} = -\tfrac{1}{2}W_{\mu\nu}^{\dagger}W^{\mu\nu} + M^2 W_{\mu}^{\dagger}W^{\mu} + iQW_{\mu}^{\dagger}W_{\nu}F^{\mu\nu}, \quad (2.1)$$

where $W_{\mu\nu} = \partial_\mu W_\nu - \partial_\nu W_\mu$ and we have included the coupling of the W to the electromagnetic field strength tensor $F^{\mu\nu}$ as in the SM.[3] The equations of motion for W when all the background fields are fixed are

$$\nabla_\nu W^{\mu\nu} - M^2 W^\mu - iQW_\nu F^{\mu\nu} = 0. \quad (2.2)$$

For the gravitational background, in this section, we consider Einstein symmetric spaces of the form [27],

$$ds^2 = h_{ab}(y)dy^a dy^b - r(y)^2 d\sigma_n^2, \quad (2.3)$$

where σ_n is an n-dimensional Einstein space with constant curvature K and

$$d\sigma_n^2 = \sigma_{ij}(x)dx^i dx^j. \quad (2.4)$$

Later we will specialize to the Schwarzschild black hole. We use indices $a, b, c, \ldots$, for the first set of coordinates, $\{y^a\}$, spanning the m-dimensional space with metric $h_{ab}(y)$; and indices $i, j, k, \ldots$, for the second set of coordinates, $\{x^i\}$, spanning the Einstein space. Furthermore, geometric quantities and differential operators on σ_n are denoted with hats. This covers several interesting cases such as $2 + n$-dimensional spherically symmetric black holes or a singly rotating black hole in $4 + n$-dimensions (Kerr, Myers-Perry, etc. ...).

To write down the equation of motion we use a decomposition of the vector field in tensorial types [27]. W_a are m scalars, with respect to σ_n, so they must obey

$$(\hat{\Delta} + \kappa_0^2)W_a = 0, \quad (2.5)$$

(κ_0^2 is the spin-0 eigenvalue). W_i is a covector field which can be decomposed into a scalar Φ, and a transverse covector W_i^T, i.e.,

$$W_i = \hat{D}_i\Phi + W_i^T, \qquad \hat{D}_i\hat{W}^{Ti} = 0, \quad (2.6)$$

where $\hat{D}_i$ is the covariant derivative on σ_n and we use an explicit hat to denote the raising of indices using σ_{ij}; i.e., note that $\hat{W}^{Ti} = -r(y)^2 W^{Ti}$. Since Φ is a scalar, it obeys (2.5). The transverse vector obeys

---

[3]In this paper, we use the particle physics convention for the signature of the metric $(+ - - - \ldots)$.

$$(\hat{\Delta} + \kappa_1^2)W_i^T = 0, \qquad (2.7)$$

where now κ_1^2 is the spin-1 eigenvalue. This decomposition allows for an expansion of the various degrees of freedom W_a, Φ, W_i^T in a basis of harmonics of the Einstein space. Furthermore, this decomposition allows for a decoupling of the field equations into an independent vector mode W_i^T, and $m + 1$ coupled scalar fields for each set of quantum numbers labeling the basis of harmonic functions. Observe, however, that not all of these modes correspond to physically independent degrees of freedom, as shown below.

III. NEUTRAL PROCA FIELD IN A SPHERICALLY SYMMETRIC BLACK HOLE

Let us now specialize to the $Q = 0$ case. We shall consider, separately, two cases according to the value of κ_0.

A. Modes with $\kappa_0 \neq 0$

Expanding the field equations with the decomposition (2.6), using conditions (2.5) and (2.7), and defining $B_a \equiv W_a - \partial_a \Phi$, we obtain

$$\frac{\kappa_0^2}{r^2} B_a - \frac{h_{af}}{r^n} \partial_b [h^{db} h^{cf} r^n (\partial_c B_d - \partial_d B_c)]$$
$$+ M^2 B_a + \partial_a \left[\frac{1}{r^{n-2}} \partial_b (r^{n-2} h^{bc} B_c) \right] = 0, \qquad (3.1)$$

$$\frac{1}{r^{n-2}} \partial_a (r^{n-2} h^{ab} B_b) - M^2 \Phi = 0, \qquad (3.2)$$

$$\left[\frac{1}{r^2}\left(\kappa_1^2 + \frac{\hat{R}}{n} \right) + M^2 + \frac{1}{r^{n-2}} \partial_a (r^{n-2} h^{ab} \partial_b) \right] \hat{W}^{Tj} = 0. \qquad (3.3)$$

We consider the spherically symmetric case with $\{y^a\} = \{t, r\}$, $|h| = 1$, h_{ab} is diagonal, $h_{tt} = -1/h_{rr} \equiv V = 1 - \mu/r^{n-1}$, and $\mu = r_H^{n-1}$. We choose units such that the horizon radius is $r_H = 1$. Since Φ is given by the second equation in terms of the other fields, it is a nondynamical degree of freedom. In four dimensions, this agrees with the fact that a spin-1 massive field has three possible physical polarizations which, in this case, will be the two dynamical scalars and the transverse vector. In higher dimensions, the transverse vector on the n sphere will contain more (degenerate) polarizations.

We can factor out the spherical harmonics through the expansion

$$B_a = \beta_a^\Lambda(y) \mathcal{Y}_\Lambda(x), \qquad \hat{W}^{Ti} = q^\Lambda(y) \mathcal{Y}_\Lambda^i(x), \qquad (3.4)$$

where Λ denotes the mode eigenvalues for the corresponding harmonic functions. Furthermore, making the ansatz,

$$\beta_t^\Lambda = e^{-i\omega t} \psi(r), \qquad \beta_r^\Lambda = e^{-i\omega t} \frac{\chi(r)}{V}, \qquad q^\Lambda = e^{-i\omega t} \Upsilon(r),$$

and using (3.1) and (3.3) we find

$$\left[V^2 \frac{d}{dr}\left(\frac{1}{r^{n-2}} \frac{d}{dr} r^{n-2} \right) + \omega^2 - \left(\frac{\kappa_0^2}{r^2} + M^2 \right)V \right]\chi - i\omega V' \psi = 0, \qquad (3.5)$$

$$\left[\frac{V^2}{r^n} \frac{d}{dr}\left(r^n \frac{d}{dr} \right) + \omega^2 - \left(\frac{\kappa_0^2}{r^2} + M^2 \right)V \right]\psi$$
$$+ i\omega\left(\frac{2V}{r} - V' \right)\chi = 0, \qquad (3.6)$$

$$\left[\frac{V}{r^{n-2}} \frac{d}{dr}\left(r^{n-2}V \frac{d}{dr} \right) + \omega^2 - \left(\frac{\kappa_1^2 + \frac{\hat{R}}{n}}{r^2} + M^2 \right)V \right]\Upsilon = 0. \qquad (3.7)$$

Thus, we obtain two second order coupled radial equations for $\{\psi, \chi\}$ and a decoupled equation for Υ. Note that $\kappa_0^2 = \ell(\ell + n - 1)$ and $\kappa_1^2 = \ell(\ell + n - 1) - 1$ with ℓ starting at zero and one, respectively. The third combination is $\kappa_1^2 + \frac{\hat{R}}{n} = \ell(\ell + n - 1) + n - 2$.

The manipulations leading to the two coupled equations above are only valid for nonzero M. In the exactly massless (Maxwell) theory, a similar calculation leads to a single decoupled equation for one of the scalar modes, which is

$$\left[V \frac{d}{dr}\left(\frac{V}{r^{n-2}} \frac{d}{dr} r^{n-2} \right) + \omega^2 - \frac{\kappa_0^2}{r^2} V \right]\chi = 0, \qquad (3.8)$$

whereas the other mode $\psi = iV d_r(r^{n-2}\chi)/(\omega r^{n-2})$ is nondynamical. Here $d_r \equiv d/dr$. The transverse mode—ruled by Eq. (3.7)—remains the same for any M; in particular, for $M = 0$, and (only) $n = 2$ it becomes equivalent to (3.8). This will be manifest in the numerical results.

B. Modes with $\kappa_0 = 0$

For the exceptional modes with $\kappa_0 = 0$, Φ does not enter the wave equation so it is a free nondynamical field. The corresponding equation for $W_a^{(0)}$ is (the superscript denotes it is the exceptional mode)

$$\frac{h_{af}}{r^n \sqrt{|h|}} \partial_b [h^{db} h^{cf} r^n \sqrt{|h|}(\partial_c W_d^{(0)} - \partial_d W_c^{(0)})]$$
$$- M^2 W_a^{(0)} = 0. \qquad (3.9)$$

When $M^2 \neq 0$, one uses an ansatz similar to the previous section to obtain a radial equation for a dynamical degree of freedom

$$\left[\frac{V}{r^n} \frac{d}{dr}\left(\frac{r^n V}{\omega^2 - M^2 V} \frac{d}{dr} \right) + 1 \right]\psi^{(0)} = 0, \qquad (3.10)$$

and a nondynamical one, $\chi^{(0)} = i\omega V/(\omega^2 - M^2 V) d_r \psi^{(0)}$. Otherwise, for $M^2 = 0$, we recover the well-known result that all the exceptional modes are nondynamical (see, e.g., [28]).

Now that we have covered all possibilities, several comments are in order. First, there is a discrete difference

between the small mass limit and the exactly massless theory since we have different sets of equations for each case. This should not be surprising since there is an extra longitudinal mode for massive vector bosons. Second, the equations for the Maxwell theory case are all decoupled, in agreement with previous work [29]. Since decoupled radial equations have been extensively studied in the literature, we will not present the details of our analysis of such modes and refer to the method in [30,31]. Thus, in the remainder of this paper, we will focus on the solution of the coupled system for the massive theory, which will be used in conjunction with the decoupled modes to obtain the full Hawking spectrum in Sec. V.

C. Boundary conditions and radial system

In this section, we start by finding a series expansion of the solution near the horizon for the coupled system $\{\psi, \chi\}$. This will be used to initialize the corresponding fields for the radial integration at $r = 1.001$. If we define $y = r - 1$, Eqs. (3.5) and (3.6) become

$$\left[M(r)\frac{d^2}{dy^2} + N(r)\frac{d}{dy} + P(r) \right]\psi + Q(r)\chi = 0, \quad (3.11)$$

$$\left[\tilde{M}(r)\frac{d^2}{dy^2} + \tilde{N}(r)\frac{d}{dy} + \tilde{P}(r) \right]\chi + \tilde{Q}(r)\psi = 0, \quad (3.12)$$

where the polynomials are defined in the Appendix. Making use of the Frobenius method to expand ψ and χ as

$$\psi = y^\rho \sum_{j=0}^\infty \mu_j y^j, \qquad \chi = y^\rho \sum_{j=0}^\infty \nu_j y^j, \quad (3.13)$$

and inserting the above two equations into Eqs. (3.11) and (3.12), we obtain

$$\rho = \pm\frac{i\omega}{n-1} \quad \text{or} \quad \rho = 1 \pm \frac{i\omega}{n-1}. \quad (3.14)$$

We want to impose an ingoing boundary condition at the horizon, so we must choose the minus sign. Furthermore, after this sign choice, the right-hand side case produces a series expansion, which is a special case of the left-hand side (where the first coefficient is set to zero), so without loss of generality we choose $\rho = -i\omega/(n-1)$. One then writes down the recurrence relations and concludes that a general solution close to the horizon can be parametrized by the two coefficients ν_0 and ν_1. The other coefficients are generated by the recurrence relations (A1).

To understand the asymptotic behavior of the waves at infinity, we now study a large r asymptotic expansion in the form

$$\psi = e^{\beta r}r^p \sum_{j=0} \frac{a_j}{r^j}, \qquad \chi = e^{\beta r}r^p \sum_{j=0} \frac{b_j}{r^j}. \quad (3.15)$$

Inserting this into Eqs. (3.5) and (3.6) we obtain, at leading order,

$$\beta = \pm ik; \quad p = 1 - \frac{n}{2} \pm i\varphi \quad \text{or} \quad p = -\frac{n}{2} \pm i\varphi, \quad (3.16)$$

where $\varphi = \delta_{n,2}(\omega^2 + k^2)/(2k)$. Thus, one can show that asymptotically[4]

$$\psi \rightarrow \frac{1}{r^{(n/2)-1}}\left[\left(a_0^+ + \frac{a_1^+}{r} + \ldots\right)e^{i\Phi} + \left(a_0^- + \frac{a_1^-}{r} + \ldots\right)e^{-i\Phi} \right],$$

$$\chi \rightarrow \frac{1}{r^{(n/2)-1}}\left[\left(\left(-\frac{k}{\omega} + \frac{c^+}{r}\right)a_0^+ + \ldots\right)e^{i\Phi} \right.$$
$$\left. + \left(\left(\frac{k}{\omega} + \frac{c^-}{r}\right)a_0^- + \ldots\right)e^{-i\Phi} \right], \quad (3.17)$$

where $\Phi \equiv kr + \varphi \log r$ and $c^\pm$ is defined in the Appendix, Eq. (A2). So as expected, each field is a combination of ingoing and outgoing waves at infinity. This asymptotic expansion also shows that for a generic wave at infinity, we can choose four independent quantities $\{a_0^\pm, a_1^\pm\}$ at infinity to characterize the solution. This is expected, since we have two coupled scalar fields and for each scalar degree of freedom we must have an associated ingoing wave and outgoing wave. Thus, we can define four new fields $\{\chi^\pm, \psi^\pm\}$ (which will asymptote, respectively, to $\{a_0^\pm, a_1^\pm\}$), by truncating the expansion for the fields and for their first derivatives at infinity. Such a transformation can be written in matrix form by defining the four-vector $\Psi^T = (\psi_+, \psi_-, \chi_+, \chi_-)$ for the new fields, and another four-vector $\mathbf{V}^T = (\psi, d_r\psi, \chi, d_r\chi)$ for the original fields and derivatives. Then, the transformation is given in terms of an r-dependent matrix $\mathbf{T}$ defined through

$$\mathbf{V} = \mathbf{T}\Psi, \quad (3.18)$$

which we provide in the Appendix, Eq. (A3). Finally, we obtain a first order system of ODEs for the new fields. First, we define a matrix $\mathbf{X}$ through

$$\frac{d\mathbf{V}}{dr} = \mathbf{X}\mathbf{V}, \quad (3.19)$$

which is read out from the original system (3.5) and (3.6). Its explicit form is given in the Appendix, Eq. (A4). Then we obtain

$$\frac{d\Psi}{dr} = \mathbf{T}^{-1}\left(\mathbf{X}\mathbf{T} - \frac{d\mathbf{T}}{dr}\right)\Psi. \quad (3.20)$$

We can write other equivalent systems using different $\mathbf{T}$ matrices. In particular, we have also integrated a first order system using the fields $\psi_s = k\psi - isd_r\psi$ and $\chi_s = k\chi - isd_r\chi$, which produced numerically equivalent results. The only difference is that for such fields we need to extract $\mathcal{O}(r^{-1})$ coefficients to obtain a_1^s.

---

[4]We have used, without loss of generality, the leading power behavior for p and discarded the second option similarly to the near horizon expansion.

IV. THE HAWKING SPECTRUM

The boundary conditions we have chosen in Sec. III C are suitable for the computation of the Hawking spectrum of radiated quanta from the black hole. The Hawking spectrum is generically given by a sum over a complete set of modes with labels ζ, of the transmission factor $\mathbb{T}_\zeta$ times a thermal average number of quanta produced at the horizon $\langle n_\zeta \rangle$. This is defined for a basis of decoupled modes. In our problem, we have a subset of modes, the transverse vector mode, and the $\ell = 0$ ($\kappa_0 = 0$) mode, which are decoupled. But we also have a tower of modes which are coupled two by two for each $\ell > 0$, the two scalars ψ and χ. It is not obvious how to decouple them for all r through an explicit transformation. Instead, let us try to understand how to extract the relevant information in the asymptotic regions.

Let us denote the two coupled fields by a two-vector $\mathbf{U^T} = (\psi, \chi)$ and represent the coupled system of radial equations through a (linear) second order matrix differential operator $\mathcal{D}^{(2)}$ acting on $\mathbf{U}$, i.e., $\mathcal{D}^{(2)}\mathbf{U} = 0$. The system is coupled because of the off diagonal elements of the $\mathcal{D}^{(2)}$ operator. To decouple the system we would have to find a transformation of the fields $\mathbf{U} = \mathcal{A}\bar{\mathbf{U}}$, such that the new differential operator $\bar{\mathcal{D}}^{(2)} = \mathcal{D}^{(2)} \circ \mathcal{A}$ is diagonal, i.e.,

$$\bar{\mathcal{D}}^{(2)} = \begin{pmatrix} \bar{\mathcal{D}}_1^{(2)} & 0 \\ 0 & \bar{\mathcal{D}}_2^{(2)} \end{pmatrix}. \tag{4.1}$$

Even without finding such a transformation explicitly, one can draw some conclusions by assuming its existence.[5] In particular, we may establish a map between our general solution of the coupled system and the actual decoupled solution, for each of the asymptotic regions (horizon and far field). To find such a map let us first summarize the information we have on the general solution of the coupled system.

In Sec. III we have found that a general solution is parametrized by 4 independent coefficients in one of the asymptotic regions, either at the horizon or at infinity. Once we have chosen one set of coefficients, say at the horizon, due to the linearity of the equations, the 4 independent wave components at infinity are a linear combination of the 4 coefficients at the horizon. Let us formally denote the ingoing and outgoing wave coefficients at the horizon $(+ / -,$ respectively) by

$$\vec{\mathbf{h}} = (\mathbf{h}^+, \mathbf{h}^-) = (h_i^+, h_i^-),$$

where $i = 1, 2$ since we have two fields. Similarly, the coefficients at infinity are defined as the large r limit of

---

the $\mathbf{\Psi}$ field components (up to linear transformation which we will define next), i.e.,

$$\vec{\mathbf{y}} = (\mathbf{y}^+, \mathbf{y}^-) = (y_i^+, y_i^-),$$

with $i = 1, 2$ for ψ and χ, respectively. Because of linearity, we can define a scattering matrix

$$\vec{\mathbf{y}} = \mathbf{S}\vec{\mathbf{h}} \Leftrightarrow \begin{pmatrix} \mathbf{y}^+ \\ \mathbf{y}^- \end{pmatrix} = \begin{pmatrix} \mathbf{S}^{++} & \mathbf{S}^{+-} \\ \mathbf{S}^{-+} & \mathbf{S}^{--} \end{pmatrix}\begin{pmatrix} \mathbf{h}^+ \\ \mathbf{h}^- \end{pmatrix} \Leftrightarrow \begin{pmatrix} y_i^+ \\ y_i^- \end{pmatrix}$$

$$= \sum_j \begin{pmatrix} S_{ij}^{++} & S_{ij}^{+-} \\ S_{ij}^{-+} & S_{ij}^{--} \end{pmatrix}\begin{pmatrix} h_j^+ \\ h_j^- \end{pmatrix}, \tag{4.2}$$

which is a set of numbers (depending on energy, angular momentum, etc.) containing all the information on the scattering process. It can be fully determined by considering specific modes at the horizon and integrating them outwards. In our problem, we have imposed an ingoing boundary condition at the horizon which is simply $\mathbf{h}^+ = 0$. Then

$$\mathbf{y}^s = \mathbf{S}^{s-}\mathbf{h}^-. \tag{4.3}$$

Taking the $s = -$ component, and denoting the inverse matrix of $\mathbf{S}^{--}$ by $(\mathbf{S}^{--})^{-1}$, we invert (4.3) to obtain the wave at the horizon given the ingoing wave at infinity

$$\mathbf{h}^- = (\mathbf{S}^{--})^{-1}\mathbf{y}^-. \tag{4.4}$$

Inserting this relation back in the $s = +$ component of (4.3), we obtain the outgoing wave in terms of the ingoing wave, at infinity

$$\mathbf{y}^+ = \mathbf{S}^{+-}(\mathbf{S}^{--})^{-1}\mathbf{y}^- \equiv \mathbf{R}\mathbf{y}^-, \tag{4.5}$$

where in the last line we have defined the reflection matrix $\mathbf{R}$. Before proceeding, we note that there is still some freedom in the definition of the asymptotic coefficients since any (nonsingular) linear combination is equally good from the point of view of satisfying the boundary condition. This freedom can be written in terms of 3 matrices $\mathbf{M}^s, \mathbf{M}_H^-$ relating some new fields (hatted) to the old fields,

$$\mathbf{y}^s = \mathbf{M}^s\hat{\mathbf{y}}^s, \qquad \mathbf{h}^- = \mathbf{M}_H^-\hat{\mathbf{h}}^-. \tag{4.6}$$

Since this represents the most general parametrization of the solution in the asymptotic regions, there must be a choice which decouples the fields in those regions. To find the correct transformation we need a physical prescription.

To obtain the transmission factor for the decoupled components, it is instructive to remind ourselves of the calculation of the transmission factor for a single decoupled field. It is defined as the fraction of the incident wave which is transmitted to the horizon. If we look at a wave with energy ω (for an observer at infinity), with ingoing/outgoing amplitudes $Y_{\mp}^{(\infty)}$, then [32]

$$\mathbb{T} = \frac{|Y_-^{(\infty)}|^2 - |Y_+^{(\infty)}|^2}{|Y_-^{(\infty)}|^2} = \frac{\omega(|Y_-^{(\infty)}|^2 - |Y_+^{(\infty)}|^2)}{\omega|Y_-^{(\infty)}|^2} = \frac{\mathcal{F}_H^{\rm in}}{\mathcal{F}_\infty^{\rm in}}, \quad (4.7)$$

where in the last step we note that $\mathbb{T}$ can be reexpressed as a ratio between the total incident energy flux $\mathcal{F}_H^{\rm in}$ (which is the difference between the energy carried by the ingoing wave and the energy of the outgoing wave) and the incident energy flux associated with the ingoing wave at infinity ($\mathcal{F}_\infty^{\rm in}$). The former is the flux of energy transmitted down to the horizon.

We now compute the energy fluxes through a sphere at radius r using the energy momentum tensor. This will allow us to identify the decoupled fields at infinity and at the horizon, and, in particular, the ingoing and outgoing decoupled waves at infinity. Such a flux is shown to be conserved in our background, by using the conservation law for the energy momentum tensor, combined with the fact that the spatial integral of $T_t^{\,t}$ for each energy eigenmode is constant. It is defined, evaluated at r, as

$$\mathcal{F}|_r = -\int_{S^n} d\Sigma\, T_t^{\,r}, \quad (4.8)$$

where $d\Sigma$ is the volume element on a $t, r =$ constant hypersurface; up to an irrelevant normalization, the energy momentum tensor for the complex neutral Proca field is

$$T^{\mu\nu} = -\frac{1}{2}(W^{\dagger\mu\alpha}W^\nu_{\,\alpha} - M^2 W^{\dagger\mu}W^\nu + c.c.) - \frac{g^{\mu\nu}}{2}\mathcal{L}. \quad (4.9)$$

If we insert this in (4.8), assume a field configuration with a well-defined energy ω, and make use of the equations of motion, then, for the nontrivial case of $M^2 \neq 0 \neq \kappa_0^2$, we obtain

$$\mathcal{F}|_r = \sum_\Lambda \frac{i\omega V Y_\Lambda^\dagger}{2r^2}\frac{dY_\Lambda}{dr} + \sum_\Lambda \left\{ \frac{\kappa_0^2}{2r^2}\psi^\dagger \chi \right.$$
$$\left. -\frac{1}{2M^2}\left[\frac{V}{r^n}\frac{d(r^n\xi^\dagger)}{dr} - \frac{\kappa_0^2\psi^\dagger}{r^2}\right]\left[i\omega\xi + \frac{\kappa_0^2\chi}{r^2}\right]\right\} + c.c., \quad (4.10)$$

where for convenience we define $\xi = d_r\psi + i\omega\chi$. Modes with different angular momentum eigenvalues are clearly decoupled, as are the transverse vector mode contributions in the first sum. The terms in the second sum couple two fields for fixed Λ. We can compute the flux at infinity and close to the horizon and express it in terms of the asymptotic coefficients in the corresponding region. Focusing on a specific mode and in the coupled part of the flux [second sum in (4.10)],

$$\mathcal{F}_\infty^{\rm coupled} = |y_0^-|^2 - |y_0^+|^2 + |y_1^-|^2 - |y_1^+|^2$$
$$\equiv (\mathbf{y}^-)^\dagger\mathbf{y}^- - (\mathbf{y}^+)^\dagger\mathbf{y}^+, \quad (4.11)$$

where y_i^s are linear combinations of the asymptotic coefficients a_i^s given in the Appendix, Eq. (A5). This choice of

y_i^s is already in a form close to decoupled, since we have separated the modulus square of the incident contribution from the reflected contribution, without interference terms. This form is invariant under separate unitary transformations of $\mathbf{y}^\pm$. Using the reflection matrix we obtain

$$\mathcal{F}_\infty^{\rm coupled} = (\mathbf{y}^-)^\dagger(\mathbf{1} - \mathbf{R}^\dagger\mathbf{R})\mathbf{y}^- \equiv (\mathbf{y}^-)^\dagger\mathbf{T}\mathbf{y}^-, \quad (4.12)$$

where we have defined a (Hermitian) transmission matrix $\mathbf{T}$. This can be diagonalized through a unitary transformation, which is the remaining freedom we have for $\mathbf{y}^-$. In fact we can do even better, and diagonalize the reflection matrix $\mathbf{R}$ with a bi-unitary transformation using the arbitrary unitary $\mathbf{M}^\pm$ transformations. Then the fields are manifestly decoupled at infinity, both at the level of the reflection matrix and the transmission matrix. As a consequence, in the decoupled basis, an incident wave is reflected back in the same decoupled mode without interference with the other mode. Finally, the transmission factors are simply the eigenvalues of $\mathbf{T}$, since they are each associated with a decoupled component.

Furthermore, one can use the conservation law for the flux, to find an alternative expression for the transmission matrix at the horizon (this will be useful to control numerical errors). The total flux at the horizon is

$$\mathcal{F}_H^{\rm coupled} = (\mathbf{h}^-)^\dagger\mathbf{h}^-, \quad (4.13)$$

where the h_i^- coefficients are linear combinations of the two independent ν_i coefficients ($i = 0, 1$), given in the Appendix, Eq. (A6). Equation (4.13) establishes the important point that the flux is positive definite, so the transmission factors must be positive definite (as expected since there is no superradiance in Schwarzschild space-time). Finally, using the relation between $\mathbf{y}^-$ and $\mathbf{h}^-$ through[6] $\mathbf{S}^{--}$, we find

$$\mathbf{T} = (\mathbf{S}^{--}\mathbf{S}^{\dagger --})^{-1}. \quad (4.14)$$

Once we have obtained the transmission factors, the number and energy fluxes are given by the standard result

$$\frac{d\{N, E\}}{dt\,d\omega} = \frac{1}{2\pi}\sum_\ell \sum_\zeta \frac{\{1, \omega\}}{\exp(\omega/T_H) - 1} d_\zeta \mathbb{T}_\zeta, \quad (4.15)$$

where ζ is a label running over the final set of decoupled scalar modes and the transverse mode, and d_ζ are the degeneracies of the corresponding spherical harmonics. Labeling the scalar and vector harmonic degeneracies by d_S and d_V, respectively, we have [33]

$$d_S = \frac{(n + 2\ell - 1)(n + \ell - 2)!}{(n - 1)!\ell!}, \quad (4.16)$$

---

[6]Note that the relation between $\mathbf{h}^-$ and $(\mathbf{M}^-)^{-1}\mathbf{y}^-$ can be made diagonal using $\mathbf{M}_H^-$, so the problem is also decoupled at the horizon.

$$d_V = \frac{(n + 2\ell - 1)(n + \ell - 1)(n + \ell - 3)!}{(\ell + 1)(\ell - 1)!(n - 2)!}. \quad (4.17)$$

The Hawking temperature in horizon radius units is

$$T_H = \frac{n - 1}{4\pi}. \quad (4.18)$$

V. RESULTS

In this section we present a selection of numerical results to illustrate the behavior of the transmission factors and the corresponding Hawking fluxes. To integrate the coupled and decoupled radial equations, we first wrote test codes in MATHEMATICA7 and then a code in the C++ language, using the numerical integration routines of the Gnu Standard Library. Besides using different programming frameworks, we have also tested different integration strategies which all agreed within relative numerical errors smaller than 0.1%. In fact, most of our numerical points have a precision which is 1 order of magnitude better. To check numerical errors, we have integrated the radial equations up to a large radius of typically $r = 10^4 r_H$ and varied this up to a factor of 3 to check the precision. Furthermore, we have used the two expressions for the transmission factor from Eqs. (4.12) and (4.14), which agree within the quoted precision for almost all energies. The exception is for small energy, where the first definition converges poorly. This can be explained by a simple analysis of the propagation of errors combined with the fact that the $\mathbf{y}^{\pm}$ coefficients grow very fast as we decrease energy, thus requiring a very large precision for some fine cancellations to occur. The second expression is thus more natural in that limit since it does not need such cancellations and does not require such large precision.

We have generated several samples of transmission factors, some of which are displayed in Fig. 1. Hereafter, we shall denominate the partial waves associated to the different modes of the Proca field by ℓ_1, ℓ_2, ℓ_T, and $\ell = 0$, where ℓ_1, ℓ_2 correspond to the two coupled modes ruled by Eqs. (3.5) and (3.6), ℓ_T to the decoupled mode described by Eq. (3.7), and $\ell = 0$ to the $\kappa_0 = 0$ mode, ruled by Eq. (3.10). Moreover, partial waves associated to the Maxwell field shall be denoted by ℓ_E, and are ruled by (3.8).

In the top row panels of Fig. 1, we show the partial wave contributions for $n = 2, 3, 4$ in the zero mass limit. Some general properties are as follows. The $\mathbb{T}_\ell$ curve becomes shifted toward higher frequencies both as ℓ is increased for n fixed, and as n is increased for ℓ fixed. The former can be understood from standard geometrical optics arguments. Moreover, for this choice there is always a numerical coincidence between one of the partial waves (ℓ_1) obtained from the two coupled fields and the electromagnetic partial wave ℓ_E. The $\ell = 0$ and ℓ_2 modes are always absent in the Maxwell theory, so they can be associated with the longitudinal polarization of the massive vector field. Similarly,

the ℓ_T and ℓ_1 partial waves are associated with the transverse polarizations of the field. A qualitative dependence on dimension is that for $n = 2$, ℓ_T and ℓ_1 (or ℓ_E) modes are all equal. Curiously, this is in agreement with the fact that they describe the same number of transverse degrees of freedom as can be seen from the degeneracies (4.16) specialized for $n = 2$. This degeneracy is lifted for $n > 2$.

For nonzero mass (middle and bottom row panels of Fig. 1), the degeneracy observed for $n = 2$ in the massless limit is lifted. Also, we observe, for all n, that modes with higher ℓ partial waves (especially ℓ_1 modes) become a more dominant contribution at lower energies, as compared to lower ℓ partial waves of other modes. In particular, for $M = 1$, the transmission factor for ℓ_1 becomes the largest for small energy. This effect of the excitation of subdominant partial waves is well known to exist, for example, as we increase n (and we can also observe such effect in our plots) as well as with the introduction of black hole rotation [34]. If this effect persists cumulatively on a rotating background, then we may have enhanced angular correlations for massive Proca fields emitted from the black hole, since higher ℓ partial waves are less uniform.

Another outstanding point is that for large mass, when $n = 2, 3$, it can be seen that the transmission factor starts from a constant nonzero value at the threshold $\omega = M$ ($k = 0$), at least for small ℓ. We have checked that this does not happen for $n \geq 4$ for masses as large as $M = 10 \sim 15$, where the curves always asymptote smoothly to zero at $k = 0$. Note that the parameter in the radial equations is M^2 so these are very large masses. A possible explanation for this phenomenon can be motivated from considerations about the range of the gravitational field in Rutherford scattering. In $n = 2$, the total cross section for Rutherford scattering diverges, so the Newtonian gravitational potential is long ranged. This means that the effective size of the gravitational potential is infinite. The same happens in $n = 3$ but only at zero momentum $k = 0$. This indicates that a possible reason is that an incident wave at infinity with a very small momentum will still be sufficiently attracted by the gravitational field so that a constant nonzero fraction is still absorbed by the potential. In particular, we note that some of the radial equations are similar in form to those obeyed by massive scalar and massive fermion fields, so the same effect exists for such fields. To our knowledge, this feature has not been noted or discussed in the literature. The only exception is the paper by Nakamura and Sato [35] in four dimensions, where it is claimed that the reflection factor for a scalar field always goes to 1 at $\omega = M$ (and thus the transmission factor goes to zero). Their result seems, however, inconsistent with Figs. 1, 2, and 3 of the paper by Page [36] (also in four dimensions), where the Hawking fluxes for massive fermions become constant at the $k = 0$ threshold (in agreement with our result).
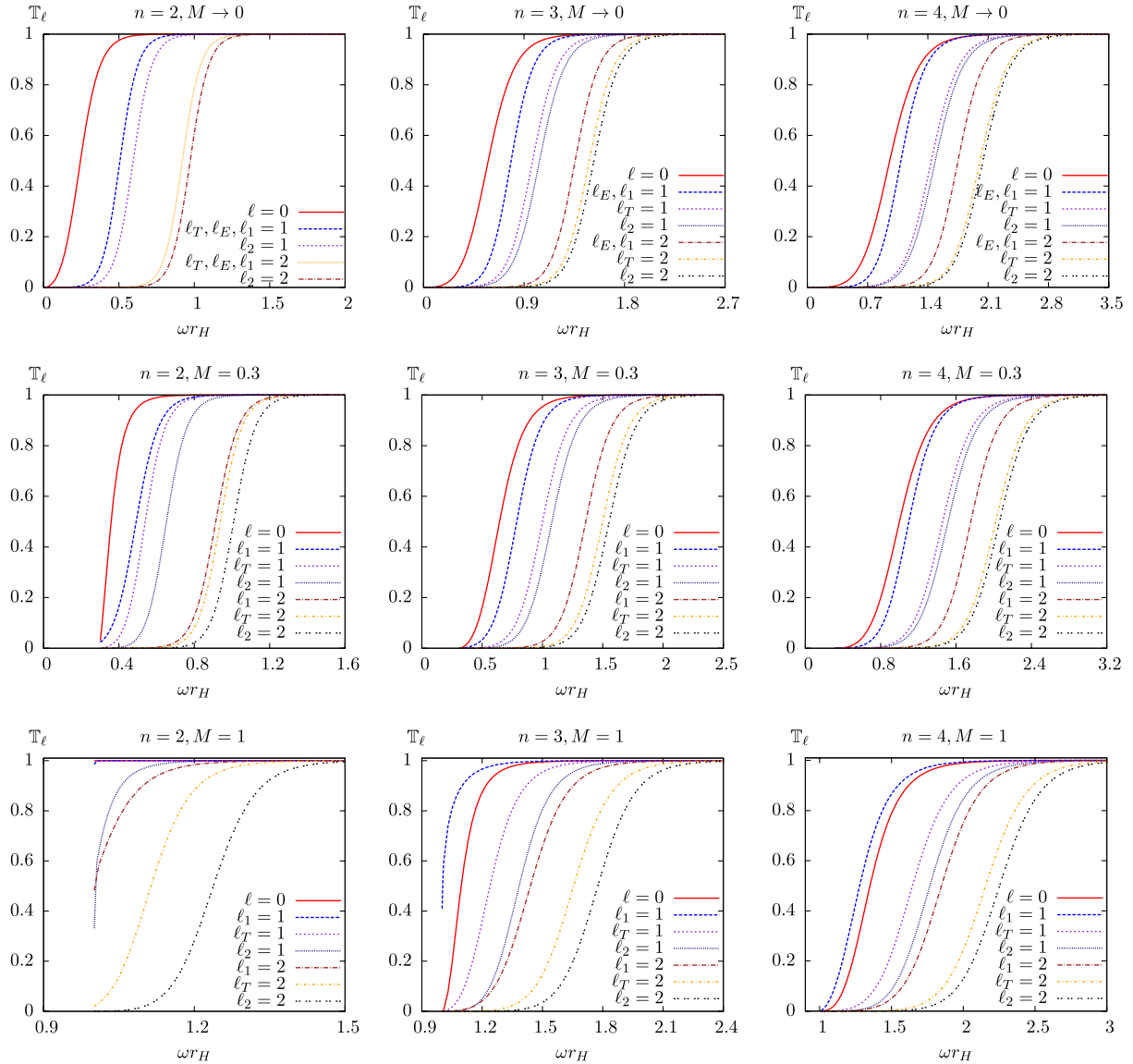
FIG. 1 (color online).   Transmission factors: The three rows of panels show the first few partial waves contributing to the Hawking spectrum. Each row corresponds to a fixed mass and each column to a fixed dimension. In particular, the first row shows the small mass limit of the Proca theory in order to compare it with Maxwell's theory.

Once we obtain the transmission factors, the computation of the Hawking fluxes (4.15) follows straightforwardly by summing up partial waves with the appropriate degeneracy factors (4.16). We have chosen to show the flux of the number of particles. The flux of energy has similar features and is simply related by multiplying each point in the plots by ω.

In Fig. 2 we compare the Hawking fluxes of the Maxwell theory with the small mass limit of the Proca theory. For the particular case of $n = 2$ we have reproduced the results by Page [37] for the electromagnetic field and found very good agreement. All panels show a red solid curve corresponding to the total Hawking flux summed up over partial waves. The partial waves in-

cluded in the sum are also represented, scaled up by the appropriate degeneracy factor. As claimed in the discussion of the transmission factors, as we increase n, partial waves with larger ℓ become more important, for both Maxwell and Proca fields. One can clearly see that there is a large contribution to the total flux from the longitudinal degrees of freedom, since the vertical scales are larger for the Proca field. In particular, the $\ell = 0$ mode enhances the spectrum greatly at small energies. Note that these extra contributions associated with the longitudinal degrees of freedom cannot, in general, (for arbitrary mass) be described by a scalar field, since there is always a contribution from the coupled modes ℓ_1, ℓ_2. That is, however, the approximation done so far in black
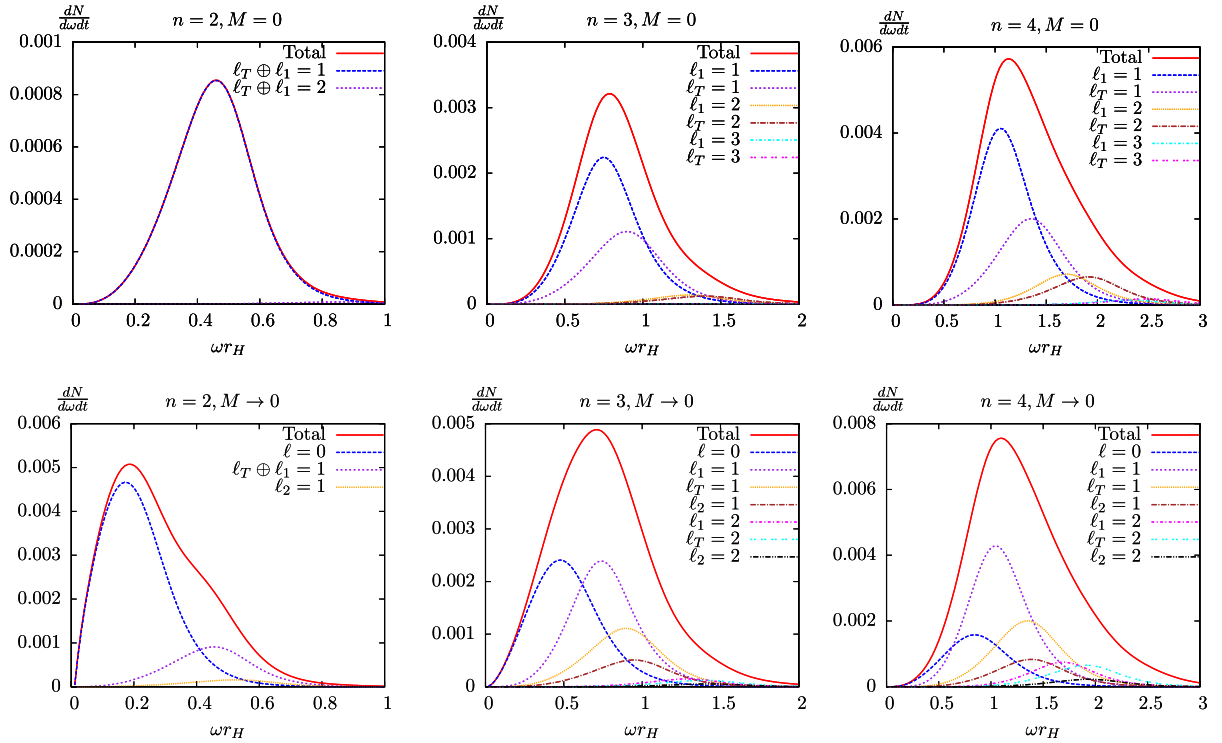
FIG. 2 (color online). Number fluxes for $M = 0$ (top panels) and $M \to 0$ (bottom panels): The red solid curve of the top panels shows the Hawking flux of particles summed over the dominant partial waves for the Maxwell theory. The different partial waves are multiplied by the corresponding degeneracies. In the bottom panels the small (but nonzero) M limit of the Proca theory is shown for comparison. The $\oplus$ symbol denotes the addition of modes which are numerically equal.

hole event generators, where the W and Z fields Hawking spectra in use are those of the electromagnetic field (for transverse polarizations) and a scalar field (for the longitudinal polarization). Thus, our results can be readily applied to improve this phenomenological modeling.

In Fig. 3, we show the variation of the total number flux with n and M. The left panel shows the expected variation with M: that the flux not only gets cut off at the energy threshold $\omega = M$, but it is also suppressed with M (the

same holds for $n > 2$). This is the same behavior as found in [30,31]. As pointed out already, in event generators massive vector particles are modeled using the Hawking fluxes for the Maxwell field and a massless scalar, with a cutoff at the mass threshold. In [30,31] it was shown that simply imposing a sharp cutoff on the fluxes of massless scalars and fermions overshoots the real amount of Hawking radiation emitted in the massive scalar and fermion channel. Qualitative inspection of our results suggests a similar effect for the W and Z channels in the
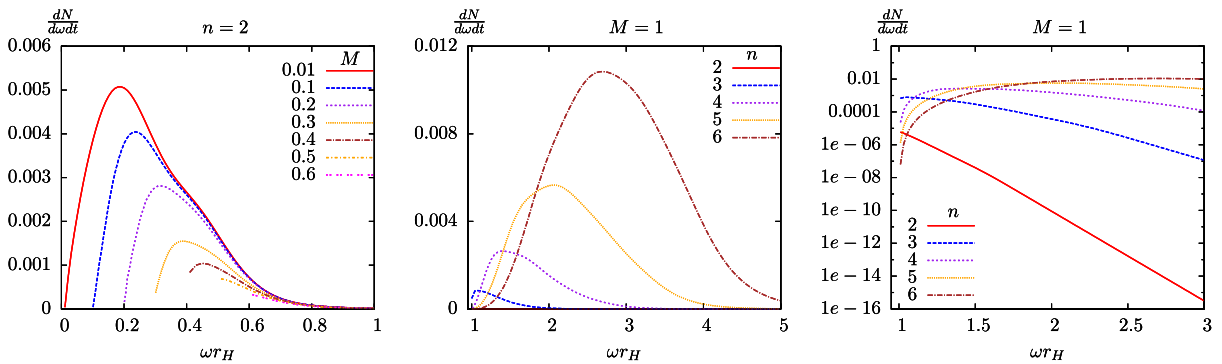

FIG. 3 (color online). Number fluxes for various M and n: (Left panel) Variation of the flux of particles for fixed $n = 2$ and variable mass. (Middle and right panels) Variation of the flux with n in a linear and logarithmic scale, respectively. The logarithmic scale shows more clearly that the limiting flux at $k = 0$ is finite for $n = 2, 3$.

evaporation. A quantitative comparison, however, requires a consideration of a Proca field confined to a thin brane. The middle and right panel show variation with n. In addition to the well-known large scaling of the area under the curve and the shift of the spectrum to larger energies, we can also see that more partial waves start contributing to the shape of the curve which becomes more wavy. This is particularly true because the degeneracy factors for fixed ℓ increase rapidly with n, which is a consequence of the larger number of polarizations available for a vector boson in higher dimensions. Finally, regarding $n = 2, 3$ we confirm the feature that the flux becomes a constant at $k = 0$. This can be seen more clearly in the right panel in a logarithmic scale where the lines for $n \geq 4$ curve very rapidly around that point, whereas for $n = 2, 3$ they tend to a constant.

VI. CONCLUSION

In this paper, we have used a numerical strategy to solve the coupled wave equations obtained in the study of a Proca field in the background of a D-dimensional Schwarzschild black hole. Our results show some expected features, such as the mass suppression of the Hawking fluxes as the Proca mass is increased, but also some novel features, such as the nonzero limit of the transmission factor, for vanishing spatial momentum, in $n = 2, 3$. Moreover, for the first time a precise study of the longitudinal degrees of freedom was carried out.

One application of our results will be to improve the model in the CHARYBDIS2 Monte Carlo event generator [22] currently in use by the ATLAS and CMS experiments. This simulates the production and decay of higher dimensional black holes in parton-parton collisions, a scenario to be soon tested at the LHC 14 TeV center of mass energy collisions. The Hawking evaporation can still be improved greatly through the numerical study of various wave equations in black hole backgrounds, which approximate the ones that could be produced at the LHC. This is illustrated by our results in this paper, which show the inaccuracy of the naive modeling of longitudinal modes by scalar fields, an approximation that has been used in event generators. For the phenomenology of TeV gravity scenarios, an important extension of the results herein is to consider a Proca field on the brane for scenarios where the vector bosons are confined within a thin brane. We hope to report on such results soon.

ACKNOWLEDGMENTS

APPENDIX: FUNCTIONS AND MATRICES

$$M(r) \equiv \sum_{m=0}^{2n-1} \alpha_m y^m = r(r^{n-1} - 1)^2,$$

$$N(r) \equiv \sum_{m=0}^{2n-2} \beta_m y^m = n(r^{n-1} - 1)^2,$$

$$P(r) \equiv \sum_{m=0}^{2n-1} \gamma_m y^m = -(\kappa_0^2 + M^2 r^2)(r^{2n-3} - r^{n-2}) + \omega^2 r^{2n-1},$$

$$Q(r) \equiv \sum_{m=0}^{2n-2} \sigma_m y^m = i\omega r^{n-1}(2r^{n-1} - n - 1),$$

$$\tilde{M}(r) \equiv \sum_{m=0}^{2n} \tilde{\alpha}_m y^m = r^2(r^{n-1} - 1)^2,$$

$$\tilde{N}(r) \equiv \sum_{m=0}^{2n-1} \tilde{\beta}_m y^m = (n - 2)r(r^{n-1} - 1)^2,$$

$$\tilde{P}(r) \equiv \sum_{m=0}^{2n} \tilde{\gamma}_m y^m = -(\kappa_0^2 + M^2 r^2)(r^{2n-2} - r^{n-1}) + \omega^2 r^{2n} - (n - 2)(r^{n-1} - 1)^2,$$

$$\tilde{Q}(r) \equiv \sum_{m=0}^{n} \tilde{\sigma}_m y^m = -i\omega(n - 1)r^n.$$

The recurrence relations are

$$\mu_0 = \nu_0,$$

$$\mu_1 = -\frac{(\rho(\rho - 1)\alpha_3 + \rho\beta_2 + \gamma_1 + \sigma_1)\nu_0 + \sigma_0 \nu_1}{\rho(\rho + 1)\alpha_2 + \gamma_0},$$

$$\mu_j = \frac{\omega^2 + (n - 1)^2(\rho + j)(\rho + j - 1)}{D_j} f_j + \frac{i\omega(n - 1)}{D_j} \tilde{f}_j,$$

$$\nu_j = \frac{\omega^2 + (n - 1)^2(\rho + j)(\rho + j - 1)}{D_j} \tilde{f}_j + \frac{i\omega(n - 1)}{D_j} f_j,$$

(A1)

with

$$D_j = (n - 1)^2 \omega^2 + (\omega^2 + (n - 1)^2(\rho + j)(\rho + j - 1))^2,$$

$$f_j = -\sum_{m=1}^{j} [(\alpha_{m+2}(\rho + j - m)(\rho + j - m - 1) + \beta_{m+1}(\rho + j - m) + \gamma_m)\mu_{j-m} + \sigma_m \nu_{j-m}],$$

$$\tilde{f}_j = -\sum_{m=1}^{j} [(\tilde{\alpha}_{m+2}(\rho + j - m)(\rho + j - m - 1) + \tilde{\beta}_{m+1}(\rho + j - m) + \tilde{\gamma}_m)\nu_{j-m} + \tilde{\sigma}_m \mu_{j-m}].$$

The coefficients used in the asymptotic expansion in the text are

$$c^{\pm} = \frac{i}{2\omega}\left[-\kappa_0^2 + \frac{n(2-n)}{4} + (2\omega^2 - M^2)(\delta_{2,n} + \delta_{3,n}) + \left(\pm i\frac{M^2}{2k} - \left(\frac{M^2}{2k}\right)^2\right)\delta_{2,n}\right]. \tag{A2}$$

The matrices used in the text are as follows:

$$\mathbf{T} = \frac{1}{r^{(n-2)/2}}\begin{pmatrix} \frac{e^{i\Phi}}{r} & \frac{e^{-i\Phi}}{r} & e^{i\Phi} & e^{-i\Phi} \\[2mm] \frac{ike^{i\Phi}}{r} & -\frac{ike^{-i\Phi}}{r} & \left[ik + \frac{i\varphi - \frac{n-2}{2}}{r}\right]e^{i\Phi} & -\left[ik + \frac{i\varphi + \frac{n-2}{2}}{r}\right]e^{-i\Phi} \\[2mm] 0 & 0 & \left(-\frac{k}{\omega} + \frac{c^+}{r}\right)e^{i\Phi} & \left(\frac{k}{\omega} + \frac{c^-}{r}\right)e^{-i\Phi} \\[2mm] 0 & 0 & \left[-\frac{ik^2}{\omega} + \frac{ikc^+ - \frac{k}{\omega}(i\varphi - \frac{n-2}{2})}{r}\right]e^{i\Phi} & -\left[\frac{ik^2}{\omega} + \frac{ikc^- + \frac{k}{\omega}(i\varphi + \frac{n-2}{2})}{r}\right]e^{-i\Phi} \end{pmatrix}, \tag{A3}$$

$$\mathbf{X} = \begin{pmatrix} 0 & 1 & 0 & 0 \\ -\frac{P}{M} & -\frac{N}{M} & -\frac{Q}{M} & 0 \\ 0 & 0 & 0 & 1 \\ -\frac{\tilde{Q}}{M} & 0 & -\frac{\tilde{P}}{M} & -\frac{\tilde{N}}{M} \end{pmatrix}, \tag{A4}$$

and the two-vectors,

$$\mathbf{y}^{\pm} = \begin{pmatrix} \sqrt{\frac{\kappa_0^2 k}{\omega}}a_0^{\pm} \\[3mm] \sqrt{\frac{\omega k}{M^2}}\left[\left(\pm i\varphi - \frac{n-2}{2} + i\omega c^{\pm} \mp ik\delta_{n,2}\right)a_0^{\pm} \pm ika_1^{\pm}\right] \end{pmatrix}, \tag{A5}$$

$$\mathbf{h}^{-} = \begin{pmatrix} \sqrt{\kappa_0^2}\,\nu_0 \\[3mm] \frac{i\omega(\mu_1 - \rho(\frac{n}{2}\nu_0 + \nu_1 - \mu_1)) + \kappa_0^2\nu_0}{M} \end{pmatrix}. \tag{A6}$$

[1] S. Teukolsky, Phys. Rev. Lett. **29**, 1114 (1972).
[2] S. Chandrasekhar, *The Mathematical Theory of Black Holes* (Clarendon, Oxford, 1992), p. 646.
[3] H. K. Kunduri, J. Lucietti, and H. S. Reall, Phys. Rev. D **74**, 084021 (2006).
[4] F. R. Tangherlini, Nuovo Cimento **27**, 636 (1963).
[5] V. Ferrari, L. Gualtieri, and S. Marassi, Phys. Rev. D **76**, 104033 (2007).
[6] C. Molina, P. Pani, V. Cardoso, and L. Gualtieri, Phys. Rev. D **81**, 124021 (2010).
[7] I. Antoniadis, Phys. Lett. B **246**, 377 (1990).
[8] N. Arkani-Hamed, S. Dimopoulos, and G. R. Dvali, Phys. Lett. B **429**, 263 (1998).
[9] I. Antoniadis, N. Arkani-Hamed, S. Dimopoulos, and G. R. Dvali, Phys. Lett. B **436**, 257 (1998).
[10] N. Arkani-Hamed, S. Dimopoulos, and G. R. Dvali, Phys. Rev. D **59**, 086004 (1999).
[11] G. 't Hooft, Phys. Lett. B **198**, 61 (1987).
[12] M. W. Choptuik and F. Pretorius, Phys. Rev. Lett. **104**, 111101 (2010).
[13] H. Yoshino and V. S. Rychkov, Phys. Rev. D **71**, 104028 (2005).
[14] C. Herdeiro, M. O. P. Sampaio, and C. Rebelo, J. High Energy Phys. 07 (2011) 121.
[15] H. Witek, M. Zilhao, L. Gualtieri, V. Cardoso, C. Herdeiro et al., Phys. Rev. D **82**, 104014 (2010).
[16] H. Witek, V. Cardoso, L. Gualtieri, C. Herdeiro, U. Sperhake et al., Phys. Rev. D **83**, 044017 (2011).
[17] H. Okawa, K.-i. Nakao, and M. Shibata, Phys. Rev. D **83**, 121501 (2011).
[18] M. Zilhao, H. Witek, U. Sperhake, V. Cardoso, L. Gualtieri et al., Phys. Rev. D **81**, 084052 (2010).
[19] H. Yoshino and M. Shibata, Phys. Rev. D **80**, 084025 (2009).
[20] S. W. Hawking, Commun. Math. Phys. **43**, 199 (1975).
[21] G. Aad et al. (The ATLAS Collaboration), arXiv:0901.0512.
[22] J. A. Frost et al., J. High Energy Phys. 10 (2009) 014.
[23] D.-C. Dai et al., Phys. Rev. D **77**, 076007 (2008).
[24] V. Khachatryan et al. (CMS Collaboration), Phys. Lett. B **697**, 434 (2011).
[25] The ATLAS Collaboration, CERN Report No. ATLAS-CONF-2011-065, 2011.

[26] The ATLAS Collaboration, CERN Report No. ATLAS-CONF-2011-068, 2011.

[27] H. Kodama, A. Ishibashi, and O. Seto, Phys. Rev. D **62**, 064022 (2000).

[28] R. Konoplya, Phys. Rev. D **73**, 024009 (2006).

[29] D. N. Page, Phys. Rev. D **13**, 198 (1976).

[30] M. O. Sampaio, J. High Energy Phys. 10 (2009) 008.

[31] M. O. Sampaio, J. High Energy Phys. 02 (2010) 042.

[32] P. Kanti, Int. J. Mod. Phys. A **19**, 4899 (2004).

[33] A. Ishibashi and H. Kodama, Prog. Theor. Phys. Suppl. **189**, 165 (2011).

[34] M. O. P. Sampaio, Ph.D. thesis, Cambridge University, 2010, http://www.dspace.cam.ac.uk/handle/1810/226741.

[35] T. Nakamura and H. Sato, Phys. Lett. **61B**, 371 (1976).

[36] D. N. Page, Phys. Rev. D **16**, 2402 (1977).

[37] D. N. Page, Phys. Rev. D **14**, 3260 (1976).